ChemistryOpen

Research Article
doi.org/10.1002/open.202200007

Chemistry
Europe
European Chemical
Societies Publishing

www.chemistryopen.org

Nanoscale Biocompatible Structures Generated from Fluorinated Tripodal Phenylenes on Gold Nanoprisms

Miguel García-Castro, Ana Moscoso, Francisco Sarabia, Juan Manuel López-Romero,* Rafael Contreras-Cáceres, and Amelia Díaz[a]

Modification of gold substrates with a stable, uniform and ultrathin layer of biocompatible materials is of tremendous interest for the development of bio-devices. We present the fabrication of hybrid systems consisting of triangular prism gold nanoparticles (Au@NTPs) covalently covered with tripod-shaped oligo(p-phenylenes) featuring trifluoromethyl groups. Their synthesis is accomplished using a biphenyl boronic ester as the key compound. Au@NTPs were prepared through a seedless procedure using 3-butenoic acid and benzyldimethyl ammonium chloride, and modified with aminothiol groups.

Coverage of this amine-modified gold substrate with a self-assembled monolayer (SAM) of tripod-shaped molecules is carried out in ethanolic solution. The hybrid system avoids up to 70% of protein corona formation, and allows unspecific attachment for bulky adsorbates, providing an optimal biosensing platform. Chemical composition and morphology are analyzed by transmission electron microscopy (TEM), UV-visible spectroscopy and field emission scanning electron microscopy (FESEM).

Introduction

Fabricating biosurfaces by modification of inorganic and polymeric surfaces with a stable, uniform and ultrathin layer of biocompatible materials is of great interest in drug delivery, biosensing, bio-devices and implantable microdevices.[1,2] The modified surfaces should present resistance or reversible adsorption of peptides, proteins and cells; in a nanoparticle biological context, they should prevent protein corona formation;[3] and they should demonstrate efficient responses towards external stimuli such as UV light, pH, temperature, magnetic fields, redox chemistry, or competitive guests. In addition, these modified substrates should offer the possibility of creating nanostructured surfaces. All of these properties can aid in mimicking the biological behavior of complex biological environments and/or allow a controlled drug release.

Hence, the design of coatings for all kind of surfaces, including that of nanoparticles (NPs), to avoid biofouling is currently an active field of research. In general, most anti-biofouling coatings should provide a neutral surface charge, the presence of hydrogen bond acceptors, absence of hydrogen bond donors, and a high hydrophilicity to promote hydration.[4] The idea behind those principles is to avoid electrostatic or hydrophobic interactions with charged patches or hydrophobic

pockets present in proteins and, on the contrary, favor the formation of a layer of water molecules right on top of the engineered surface that will hamper protein adhesion.[5] Nonetheless, there are anti-biofouling surfaces and materials that do not comply to all four of those principles and yet repel the adhesion of biomolecules, such as polyglycerols[6] or polysaccharides,[7] that have many hydrogen bond donors or form superhydrophobic surfaces.[8] In this respect, structures bearing poly(ethylene glycol) moieties have emerged as the most widely used materials for the fabrication of such bioresistant coatings.[9–14] Grafting oligo- or poly(ethylene glycol) onto surfaces has been mostly based on siloxane chemistry using trichloro- or trialkoxysilane derivatives, mainly for silicon and modified silicon surfaces,[2,15–17] and bulk blending is considered as one of the most effective and straightforward ways to prepare polymeric biomaterials by surface modification. However, these adsorbates do not offer the possibility of creating non-randomized nanostructured surfaces.

Self-assembled monolayers (SAMs) have been widely used in surface modification to create platforms for the study of biological interactions and assembly of biomolecular structures down to the nanoscopic scale. For example, SAMs have been used for studies involving enzymatic processing of DNA,[18,19] DNA computing,[20] protein assays,[9,10] studies of cellular responses towards surfaces,[21–23] or for fabricating protein- and oligosaccharide-functionalized chips in proteomics- and glyco-mics-based research.[24–26] As mentioned, with the ever increasing drive towards smaller sample sizes and higher throughput for whole-organism analysis, the need to develop nanometer-scale, biomolecular patterned surfaces has arisen.[3,27,28] However, in order to further exploit SAM-based systems in this context, i) convenient strategies for the synthesis of molecules that are tailored towards specific applications, ii) controlling non-specific adsorption of biomolecules, and iii) nanostructuration control, are required.[29] To achieve these goals, the

[a] Prof. Dr. M. García-Castro, Prof. Dr. A. Moscoso, Prof. Dr. F. Sarabia,
Prof. Dr. J. M. López-Romero, Prof. Dr. R. Contreras-Cáceres, Prof. Dr. A. Díaz
Departamento de Química Orgánica
Universidad de Málaga
Facultad de Ciencias
29071 Málaga (Spain)
E-mail: jmromero@uma.es

ChemistryOpen

Research Article
doi.org/10.1002/open.202200007

Chemistry Europe
European Chemical
Societies Publishing

physicochemical properties of the engineered SAMs surfaces, such as their size, shape, charge, hydrophobicity, or roughness, need to be defined.[30,31]

Fluorinated molecules and fluorine-oligomers can avoid undesired protein adsorption and platelet adhesion. There are numerous reports dealing with hydrophobic surface preparation methods with perfluorinated alkyl chains, due to their interesting non-fouling properties.[32–34] In fact, more than non-fouling, these surfaces are described as self-cleaning, because biomolecules do adhere, but they are easily removed by the intrinsic nature/features of the surface.[1] This is particularly interesting for marine coatings,[35] surgical equipment,[36,37] microfluidic devices,[38] and the textile industry.[39] For instance, cotton was covered with silica and TiO_2, and modified with alkyl chains containing eight perfluorinated carbon atoms to confer hydrophobicity to the surface.[39] As the fluorine content on the surface increased, so did the hydrophobicity, but only up to a point, after which the excess of coating presumably altered the roughness of the surface and the contact angle decreased slightly.[39]

Fluorinated amphiphilic polymers have been designed as promising anti-fouling coatings for surfaces.[40,41] Controlling the ratio of hydrophilic (2-hydroxyethyl methacrylate) and fluorinated (2-perfluorooctylethyl methacrylate) patches in the copolymer, protein adhesion for bovine serum albumin and human fibrinogen could be avoided.[42] Indeed, by using a percentage of hydrophilic hydroxyl moieties from 4% to 7% and fluorinated moieties ranging from 4% to 14%, protein adhesion was prevented.[43]

Therefore, fluorinated groups can have an anti-fouling effect. However, it is difficult to translate the effect to fluorinated NPs for in vivo bio-applications, as they need to somehow be hydrophilic or water-dispersible. In addition, the curvature of NPs as opposed to flat surfaces can obviously affect the interactions with biomolecules and the performance of fluorinated moieties. Not many NPs with fluorine atoms exposed on the surface have so far been reported in a biological context and their interactions with proteins have scarcely been studied. For instance, fluorinated quantum dots (QDs) of a 5 nm core diameter have been used to trap enzymes through hydrophobic interactions,[44] for which it could be expected that those fluorinated QDs may form a protein corona.[45]

Fluorinated NPs with 3 kDa PEG linkers were used to study protein corona formation through ^{19}F-based diffusion nuclear magnetic resonance (NMR) spectroscopy.[46] Changes in the diffusion coefficients (and hence in the size) of several fluorinated gold NPs were monitored by exposing them to single proteins, such as human serum albumin, but also to more complex media, such as blood, plasma, or cells. When those NPs had their fluorine atoms exposed, no size increase was detected.[46] Hence, the fluorine atoms somehow influence the NP-protein interactions. Surprisingly, even though fluorinated moieties can in principle attract proteins through hydrophobic interactions, they are available to interact and cross several biological barriers precisely benefiting from that hydrophobic character. In any case, the role of fluorine on NPs in

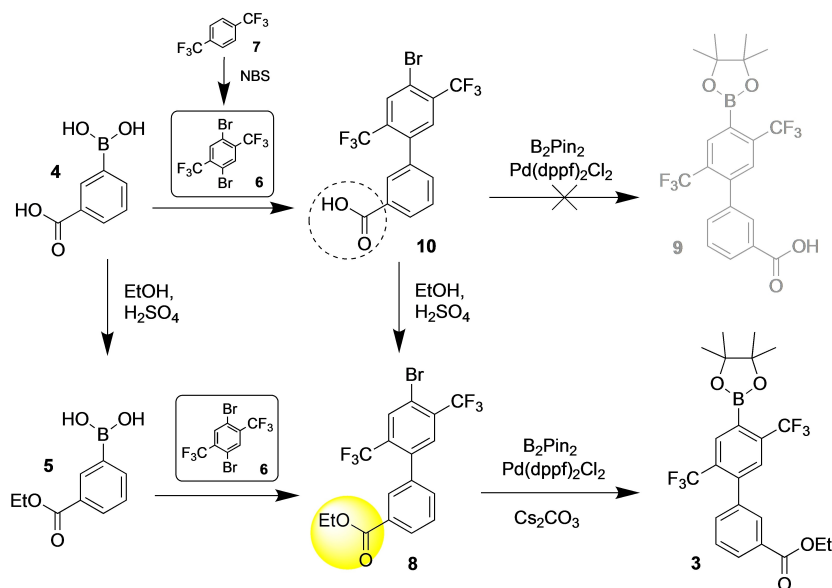protein corona formation and how this affects interactions with cells is yet to be unveiled.[46]

Regarding the nanostructuration of SAM surfaces to generate highly ordered SAMs with a high control of the orientation of the functional moieties, several shape-persistent and self-standing molecules have been developed, including: i) "molecular caltrops" with four phenylacetylene legs extending from either a tetrahedral silicon core,[47,48] or from an adamantane core,[49–51] ii) conically shaped dendron adsorbates with a functional group at the core,[52,53] and iii) tripod-shaped oligo(p-phenylenes) connected through a single silicon atom,[54,55] to be used for the functionalization of different surfaces. However, in this context, ordered macromolecular SAMs with high resistance to the non-controlled protein adsorption, should be still addressed. In this paper, we report the preparation of nanostructured and biocompatible SAMs surfaces on gold nanotriangular prisms by using oligo(p-phenylenes) containing trifluoromethyl units as adsorbates. Modified gold nanoprisms are resistant to the protein corona formation, but at the same time, they allow specific protein interaction on the surfaces. The synthesis of the adsorbates is also explored. The SAMs generated are characterized with a suite of surface analyses techniques. We also show the suitability of these materials for nanofabrication.

Results and Discussion

Synthesis

Two tripodal molecules (**1** and **2**) were prepared for comparison purposes, having three and two, respectively, phenylene groups in each leg. Compound **1** presents ethyl ester as end-capped groups and is laterally substituted by trifluoromethyl groups. These groups can be readily converted to acyl chloride groups previously to the covalent attachment to the gold surface. The fluorine substitution pattern in **1** will avoid non-specific interaction with protein molecules, providing to the structure high degree of biocompatibility for biomedical applications. It is known that oligo(phenylene) tripod-shaped molecules interact nonspecifically with protein molecules due to the hydrophobic tripod framework, thus interfering with the specific interaction of target molecules with a ligand on the focal point of the tripod. To overcome the biofouling problem, we have designed a tripod-shaped molecule with trifluoromethyl groups, **1**.

To carry out the synthesis of tripod **1**, we first prepared the biphenyl building block **3**. This compound was synthesized in three steps with a good global yield of 33% from boronic acid **4** (Scheme 1). Esterification of **4** afforded **5**. The coupling of **5** with dibromo compound **6**, which was obtained by bromination of p-bistrifluoromethyl compound **7** with NBS, under Suzuki biaryl coupling conditions provided the biphenyl **8**.[56] Then, biphenyl **8** was treated with bis(pinacolate)diboron in the presence of cesium carbonate and $Pd(dppf)_2Cl_2$ as catalyst in DME to provide **3** in good yield. Initially, the synthesis was planned by having **9** as key compound.[57] However, even when the Suzuki coupling of boronic acid **4** with **6** allowed the

ChemistryOpen

Research Article
doi.org/10.1002/open.202200007

Chemistry Europe
European Chemical
Societies Publishing

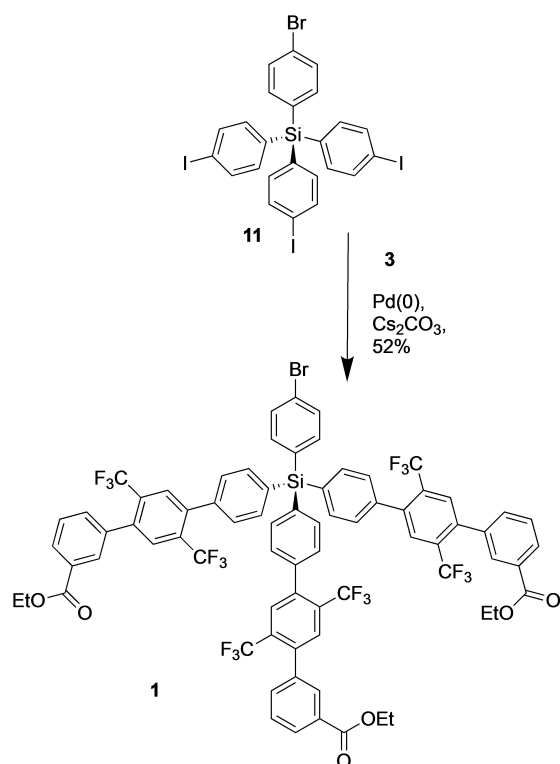**Scheme 1.** Synthesis of biphenyl building block **3**.

preparation of the biphenyl **10**, any attempt at preparing bispinacolate **9** was unsuccessful, probably due to the presence of the carboxyl group in this molecule.

Coupling of boronic ester **3** with triiodide **11** under palladium catalysis afforded the tripod **1** in good yield (52%, Scheme 2). The conversion of ethyl ester groups of **1** to chlorine atoms (–COOEt to –COCl) by hydrolysis and thionyl chloride treatment was carried out just before to the gold surface

modification (see Experimental Section). Compound **1**-COCl was not isolated. We chose the acyl chloride derivative of *p*-triphenylene as anchoring group since it can easily react with amine groups.

Additionally, a thioacetate functionalized smaller tripod (**2**) was prepared from the previously reported compound **12**.[58b] Deprotection of TBDMS groups was carried out with TBAF to afford **13**, which, under Mitsunobu conditions, afforded **2** (Scheme 3). Deprotection of thioacetate groups with triethyl-amine was carried out in situ during the gold surface modification.
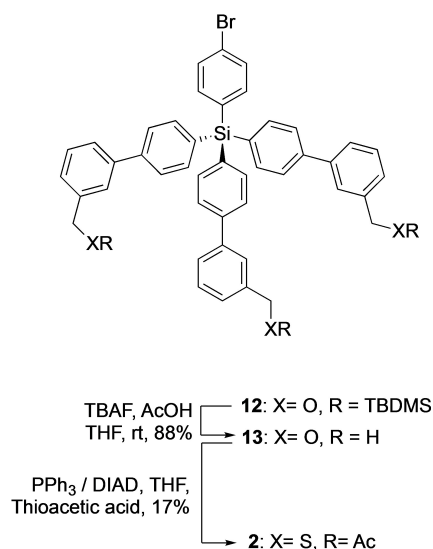
In compound **2**, designed for direct modification of gold surfaces, the presence of the thioacetyl-protecting group offers a significant improvement regarding the storage and handling of the molecules, preventing their oxidation or polymerization through intermolecular disulfide bonds. On the other, hand tripod **1** presents an acyl chloride substitution as anchoring groups, chosen for amine modification of gold nanoprisms.

Preparation of Au@NTP and Surface Modification (Au@NTP-S-NH-1 and Au@NTP-S-2)

Gold nanotriangular prisms (Au@NTPs) were prepared by following the seedless procedure, using 3-butenoic acid (3BA) and benzyldimethyl ammonium chloride (BDAC). Au@NTPs were obtained in a mixture with gold nanooctahedra and separated by depletion-induced flocculation.[59] In order to completely characterize the morphology of the obtained particles, they have been analyzed by TEM and FESEM (Figure 1). A 185 ± 7 nm average for the edge length and 32 ± 3 nm as averaged thickness have been found. Figures 1A–C show TEM images of the purified Au@NTPs, where only a few octahedral and spherical morphologies can be seen (less than 1 and 2%, respectively). Figures 1 D and E show representative

Scheme 2. Synthesis of tripod-shaped molecule **1**.

ChemistryOpen

Research Article
doi.org/10.1002/open.202200007

Chemistry
Europe
European Chemical
Societies Publishing

Scheme 3. Synthesis of tripodal compound 2.

tilted FESEM images where the morphologies of Au@NTPs nanoparticles can be clearly discerned.

For tripod 1-surface covalent modification, Au@NTPs were covered by a layer of amino alkanethiol by following the reported procedure.[60] Amino-terminated Au@NTP-S-NH$_2$ were obtained by treatment of the previously fabricated nano-particles with 6-aminohexanethiol, Briefly, Au@NTPs were dispersed in BDAC and then treated with 6-aminohexanethiol at 20 °C to give AuNTP-S-NH$_2$ dispersed in water (Figure 2).

Optical properties of the Au@NTP were measured by UV-vis spectroscopy. The Au@NTPs exhibit a maximum at 554 nm, while Au@NTP-S-NH$_2$ present a maximum at 560 nm (Figure 3F). Sharp maxima in the UV-Vis spectra of both samples, before and after aminothiol treatment, confirmed that Au@NTP-S-NH$_2$ did not lose the corners and edges of the nanotriangular prism shape.[60] This fact can be attributed to the low concentration of BDAC and the Au@NTPs used during aminothiol modification.

Coverage of amine modified gold substrates by a SAM of tripod 1 was carried out by treatment of a suspension of AuNTP-S-NH$_2$ in ethanol with a solution of compound 1, also in ethanol, for 48 h at 20 °C, to obtain Au@NTP-S-NH-1 (Figure 2). The morphology and chemical composition of Au@NTP-S-NH-1 samples were analyzed by TEM/EDX and XPS techniques. Figure 3 includes an HAADF-TEM image of 1-modified Au@NTP. A good particle distribution with monodisperse Au@NTP-S-NH-1 can be observed. The morphology of the functionalized Au@NTPs remained unmodified after coverage with the amino-thiol compound and 1, as observed in the EDX/TEM mapping analysis (Figure 3A, HAADF). As shown, for 1-modified gold nanoprisms, the EDX analysis confirmed the presence of gold, fluorine, bromine and sulfur (Figures 3B–E, respectively), thus
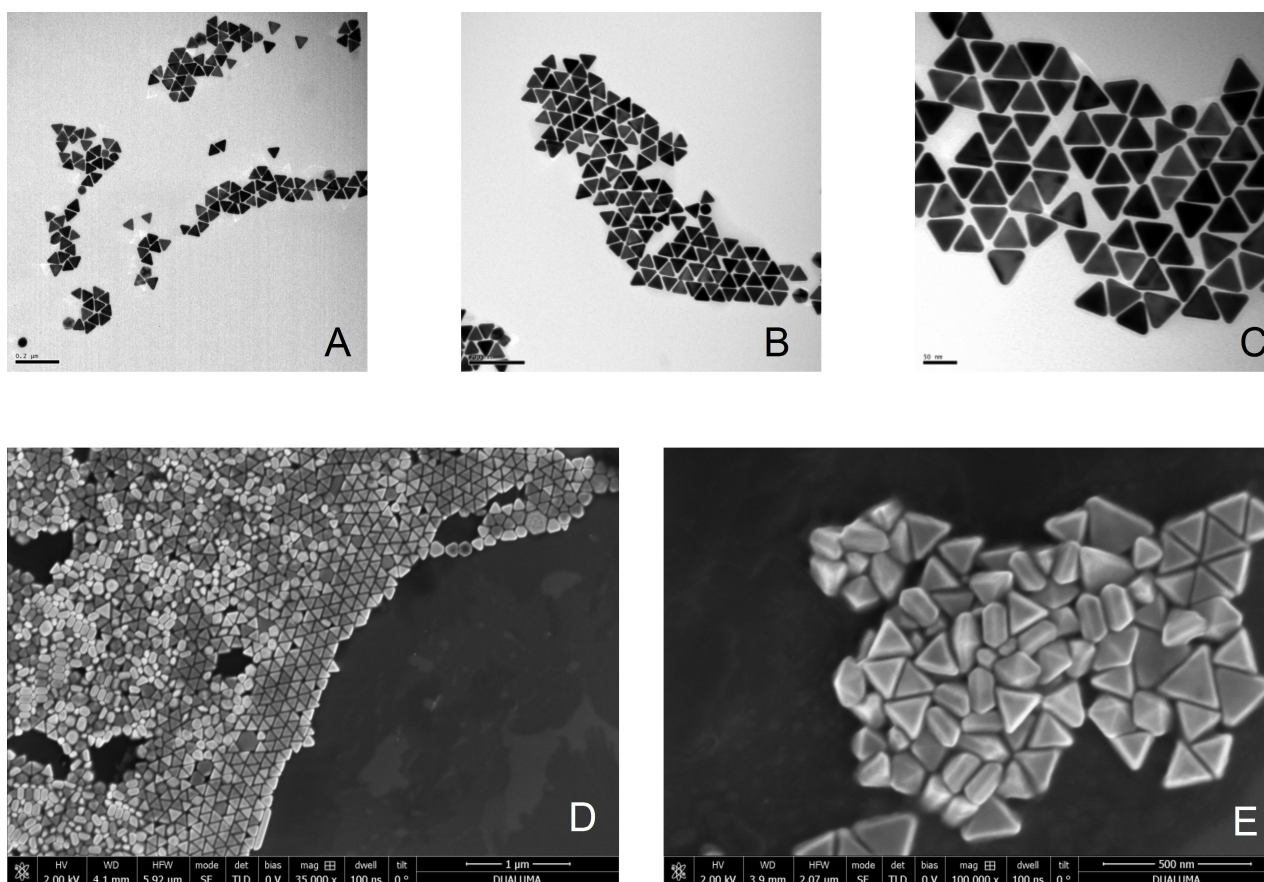

Figure 1. A–C) TEM images of the gold nanoparticles synthesized; D, E) tilted FESEM images of the Au@NTPs.
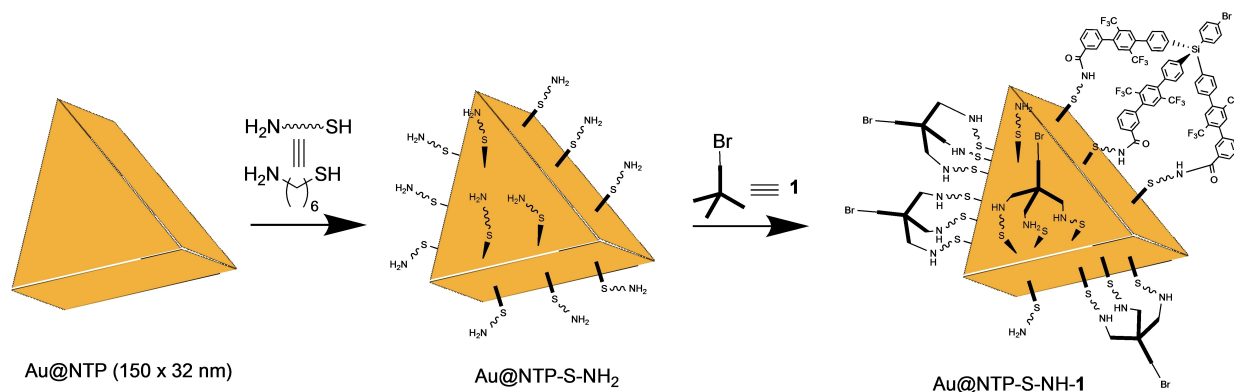
ChemistryOpen

Research Article
doi.org/10.1002/open.202200007

Chemistry
Europe
European Chemical
Societies Publishing

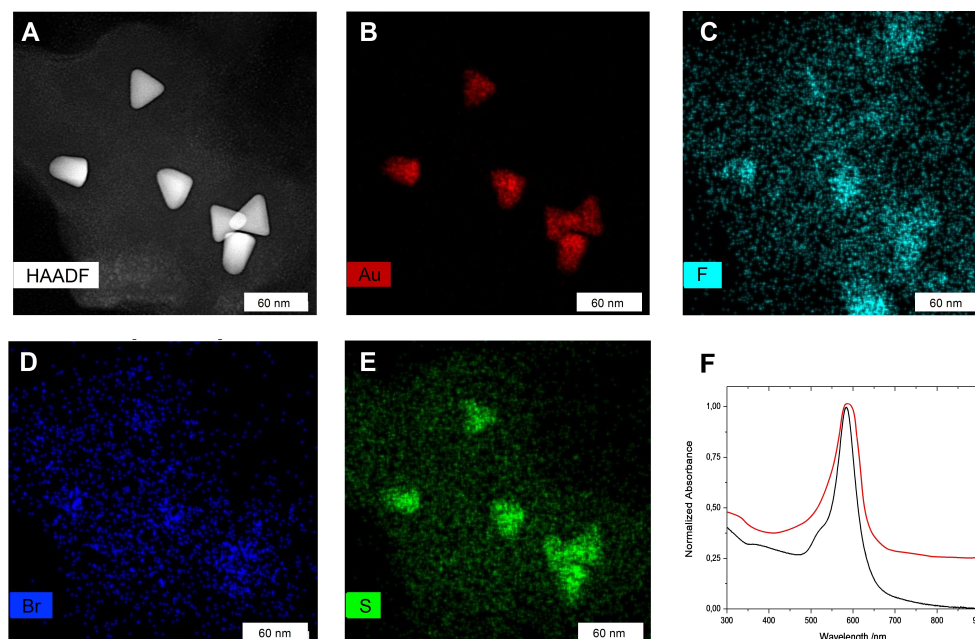**Figure 2.** Schematic representation of preparation of Au@NTP-S-NH-**1** particles.

Figure 3. A) HAADF-TEM image for **1**-modified gold nanoprisms; B), C), D), and E) EDX/TEM elemental mapping for gold, fluorine, bromine and sulfur of Au@NTP-S-NH-**1**; F) UV-vis spectrum for Au@NTP (black line) and Au@NTP-S-NH$_2$ (red line).

suggesting the presence of the molecule **1** on the amine modified gold nanoprisms. The presence of sulfur is due to the incorporation of thiol group from 6-aminohexanethiol, while the presence of fluorine and bromine can be attributed to the tripod **1**. In Figure 3C, a homogeneous distribution of fluorine can also be seen, in turn representing such distribution of compound **1** onto the gold surface.

The C1s XPS data for the resulting films of **1** are presented in Figure 4. These spectra exhibit a main peak at a binding energy of 284.0–284.4 eV, which is predominantly associated with the three tris(p-phenylene) groups of this molecule. The full width at half maximum (fwhm) of the main component peak, characteristic of the film heterogeneity, is similar to that reported for tetra(p-phenylene) tripods, which suggests a similar structural homogeneity and quality for the **1**-SAMs,[61a] with random aggregates almost absent, and with a high amount of tripods attached by the three legs. The thicknesses

of the **1**-SAMs was estimated at 1.87 nm, which is close to the calculated height of **1** upon adsorption in the desired tridentate fashion. DFT-optimized geometries for tripod **1** give a calculated height of 21.1 Å from its base and once it is attached to the surface. The thickness of the SAM prepared with **1** on the amine-modified gold surface, measured by ellipsometry, was established as 25 Å.

Correspondingly, the calculated height of **1** (distance from the base of the tripod to the ethyl ester group) is higher when attached to the surface (21.1 Å) than when calculated in solution (25.1 Å). This fact can be attributed to a more rigid configuration when the position of the three legs is fixed to the surface. In any case, the calculated height is in concordance with the measured tripod **1** height of 1.87 nm attached to the gold surface. Moreover, effective packing density of the **1** SAM prepared was estimated at approx. 1.7×10^{14} molecules cm^{-2};

ChemistryOpen

Research Article
doi.org/10.1002/open.202200007

**Chemistry
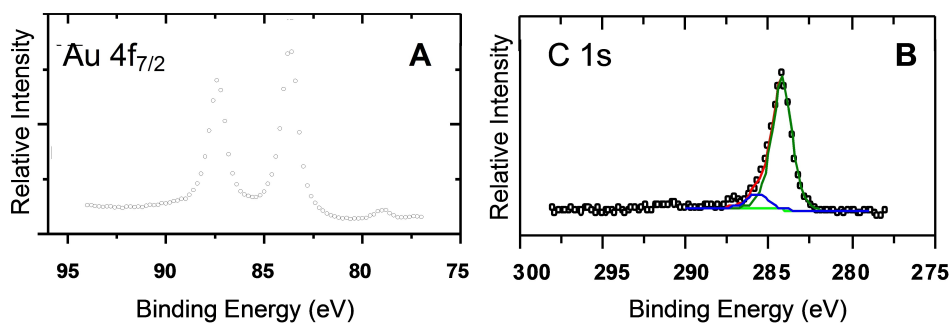Europe**
European Chemical
Societies Publishing

Figure 4. A) Au 4f$_{7/2}$ and B) C 1s XP spectra of the Au@NTP-S-NH-**1**.

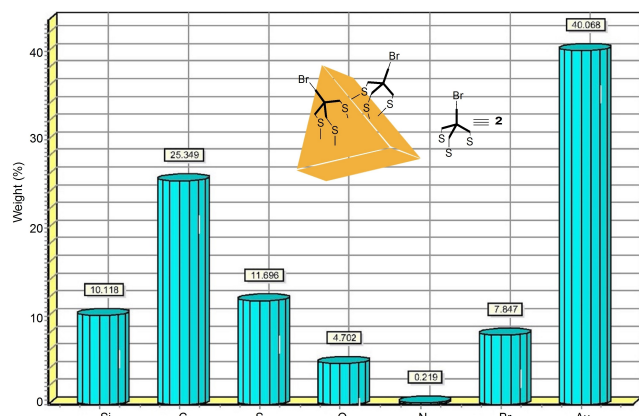this value is quite reasonable and similar to that reported for another type of tripods assembled on Au(111).[61]

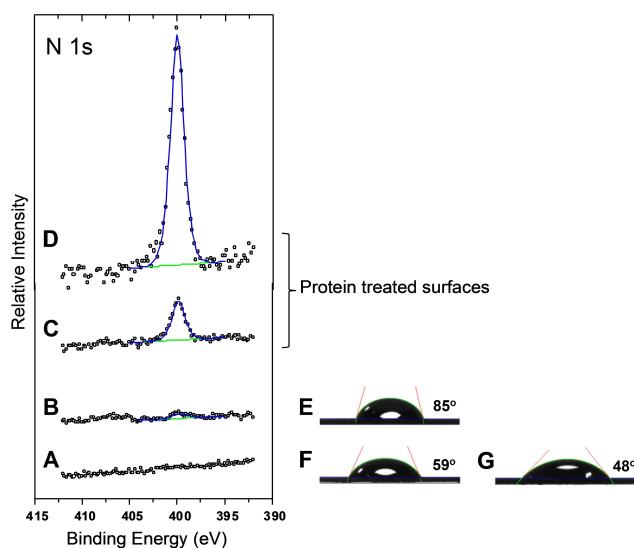**Figure 5.** Mass percentage obtained by plasma-SNMS for Au@NTP-S-**2** sample.

Figure 6. Left: N1s XP spectra of A) pristine Au@NTP, B) pristine Au@NTP-S-NH-**1**, C) Au@NTP-S-NH-**1** treated with fibrinogen, and D) Au@NTP treated with fibrinogen; right: photographs (side view) of water droplets on E) Au@NTP-S-NH-**1**, F) Au@NTP and G) Au@NTP-S-NH$_2$ surfaces in air.

On the other hand, the presence of tripod **2** on the gold surface of sample Au@NTP-S-**2** was confirmed by plasma-SNMS depth profiling. This technique has become an excellent method to obtain elemental chemical composition of thin layers of organic compounds. Results are shown in Figure 5. Au is the major component, while C, Si, S and Br are also found in Au@NTP-S-**2** confirming the presence of **2** in this system. The presence of N in the sample can be attribute to residual triethylamine.

Biocompatibility

Previously to the protein treatment, wettability of the prepared surfaces was analyzed by contact angle measurements. The water contact angles images are shown in Figures 6E–G. The presence of hydrophilic amino terminal groups in Au@NTP-S-NH$_2$ sample decreases the contact angle of the Au@NTP sample from 59° to 48° (Figures 6F and G, respectively), probably due to the formation of hydrogen bonds with water. Even when the obtained value of 59° for Au@NTP is close to angles values previously reported for gold surfaces (70°),[60] the observed difference can be explained assuming that heterogenicity of the sample can slightly decrease the contact angle value when compared with larger surfaces. The incorporation of fluorinated tripod **1** to the surface, Au@NTP-S-NH-**1** sample, renders the surfaces significantly more hydrophobic, indicated by angles reaching 85° (Figure 6E).

To examine the protein adsorption properties, the samples Au@NTP, Au@NTP-S-NH-**1** and Au@NTP-S-**2** were immersed into a slowly stirred 0.1% solution of fibrinogen in 0.01 M phosphate-buffered saline (PBS) at pH 7.4 and at 30 °C for 1 h. The samples were then washed several times with water for removal of non-adsorbed proteins and salts, followed by drying with a stream of N$_2$. For comparison, freshly prepared gold nanoprisms (Au@NTP) were also subjected to the above conditions. Results were analyzed by ellipsometry and N1s XPS techniques.

As expected, fibrinogen readily adsorbs on the gold surface of Au@NTP, resulting in a film with an ellipsometric thickness of 60 Å, corresponding to a full monolayer of fibrinogen.[17] Monolayers of 6-aminohexanothiol on gold, sample Au@NTP-S-NH$_2$, still adsorb substantial amounts of the protein, as shown

ChemistryOpen

Research Article
doi.org/10.1002/open.202200007

**Chemistry
Europe**

European Chemical
Societies Publishing

by a large increase of water contact angles and ellipsometric thickness (approx. 40 Å) corresponding to 70% of the monolayer of protein. In contrast, the corresponding **1**-terminated SAMs on nanoprisms, Au@NTP-S-NH-**1** sample, reduce adsorption of fibrinogen up to 12% monolayer formation.

The protein adsorption was also monitored by XPS based on the characteristic N1s peak (representative spectra are shown in Figures 6A–D).[62] Assuming a full monolayer adsorption of fibrinogen on Au@NTP, the integral ratio ($I_{Au@NTP-S-NH-1}$/$I_{Au@NTP}$) of the integrated areas of the N1s peaks at approx. 401 eV, arising from the adsorbed protein on the Au@NTP-S-NH-**1** sample ($I_{Au@NTP-S-NH-1}$) and Au@NTP ($I_{Au@NTP}$) corresponds to the degree of protein adsorption on the tripod modified surface. This method gives 8% monolayer adsorption of fibrinogen on the **1** film. The higher value measured by ellipsometry may be due to the errors associated with the adsorption of water and the change of reflective index of the films upon protein adsorption. In contrast, the N1s XP spectrum of the pristine Au@NTP (Figure 6A) does not exhibit any signal, and the intensity of this signal in the spectrum of Au@NTP-S-NH₂ is comparably low (Figure 6B), the intensity of the N1s signal in the spectrum of Au@NTP-S-NH-**1** treated with fibrinogen is also very low (Figure 6C) compared to that of Au@NTP treated with the protein (Figure 6D), highlighting the resistance of Au@NTP-S-NH-**1** to fibrinogen adsorption and hence to protein corona formation. Results for protein adsorption on Au@NTP-S-**2** are similar to that found for Au@NTP, showing a strong interaction among phenylene rings and fibrinogen.

Conclusion

In summary, two novel oligo(*p*-phenylene) tripod-shaped molecules have been synthesized (**1** and **2**). Both molecules present a general tetrahedral-like geometry and potential tripodal-type adsorption mode upon monomolecular assembly on gold substrates. The three legs of these molecules are terminated by thioacetate or ethyl ester groups, mediating thiolate- or amide-type anchoring to a gold or amine modified gold substrate, respectively. Compound **1** is laterally substituted with trifluoromethyl groups. SAMs of **1** on gold nanotriangular prisms have readily been prepared on amino alkanethiol-modified surfaces using an in situ generated **1**-acyl chloride derivative. The coverage of the tripod films was estimated to be about 0.37–0.39 molecules per surface gold-atom.

The presence of compound **1** gold nanoprisms in Au@NTP-S-NH₂-**1** reduces the absorbed monolayer of the model protein (fibrinogen) up to 70%. The separation between the tail groups, defined by the dimensions of the tripod-shaped molecule, is large enough compared to that in conventional monodentate-anchored SAMs. This fact allows unhindered attachment for bulky adsorbates on the tripod-modified nanoparticle, which, combined with the protein resistance of generated surface, should provide an optimal nanosystem for sensing interaction in biological media.

Experimental Section

General

Diethyl ether, dimethoxyethane (DME) and tetrahydrofurane (THF) were distilled from sodium/benzophenone under argon atmosphere, while dichloromethane (DCM) was distilled over CaH₂. All other reagents and solvents were purchased from commercial sources and used without further purification. All solvents were evaporated at reduced pressure by using a rotary evaporator. Compounds **11** and **13** were obtained according to published procedures.[58] Millipore water was used in all experiments.

Mass spectrometry (MS) measurements were carried out using electrospray ionization (ESI) or matrix-assisted laser desorption ionization time-of-flight (MALDI-TOF) technique. Samples for MALDI-TOF MS were prepared in a 2,5-dihydroxybenzoic acid (DHB) matrix. Plasma-SNMS (Secondary Neutral Mass Spectrometry) system for thin films analysis, was carried out in a Mass Spectrometer QMA 410, differentially pumped with secondary electron multiplier (SEM) detector, and a mass range of 0–340 amu. Detection limit is about 1 ppm at operating pressure or 2.3×10^{-3} atm. Plasma is obtained by using ions from inert gas (such as Ar^+, Kr^+).

¹H and ¹³C NMR spectra were recorded with a 400 MHz ARX 400 Bruker spectrometer by using the residual solvent peak in CDCl₃ (δ 7.24 ppm, 400 MHz, for ¹H and $\delta = 77.0$ ppm, 100 MHz, for ¹³C). The multiplicity of the signals is indicated as: s (singlet), d (doublet), t (triplet), q (quadruplet), m (multiplet) and for any of them, br (broad). Coupling constants *J* are given in Hertz (Hz). TLC analyses were performed on Merck silica gel 60 F 254 plates and column chromatography was performed on silicagel 60 (0.040–0.063 mm).

The surface analysis of the surface-modified materials was investigated by X-Ray photoelectron spectroscopy (XPS). XPS for gold substrates were performed with a PHI 5701 X-ray photoelectron spectrometer equipped with a monochromatic Mg Ka radiation (300 W, 15 kV, 1253.6 eV). The spectrometer was operated in the constant pass energy mode at 29.35 eV. Electron binding energies were calibrated with respect to the Cu2p3/2, Ag3d5/2 and Au4f7/2 photoelectron lines at 932.7, 368.3 and 84.0 eV, respectively. The pressure in the analysis chamber was maintained lower than $5 \cdot 10^{-6}$ Pa.

Static contact angles were performed on a goniometer model DSA25 (Krüss GmbH, Germany). The drop size of the test liquid was controlled to be 3 µL. Ellipsometry measurements were carried out in a commercial variable-angle spectroscopic ellipsometer (VASE) (J. A. Woollam Company) with a BK7 dove prism. Samples of Au@NTPs were immobilized on the gold substrate in water, these samples were mounted on the dove prism using micro-fluidic flow cell.

Field emission scanning electron microscopy (FESEM) images were obtained in a Helios Nanolab 650 Dual Beam from FEI, working at an acceleration voltage of 15 kV, a current intensity of 0.2 nA and a tilting angle of 52°. Samples were prepared by dropping 20 µL of an aqueous colloidal solution onto a 1×1 cm single side polished boron-doped silicon (111) wafer (WRS Materials).

Synthesis

Synthesis of 1,4-dibromo-2,5-bis(trifluoromethyl)benzene (**6**). 1,4-Bis(trifluoromethyl)benzene (**7**, 5 g, 23.4 mmol) was dissolved in trifluoroacetic acid (40 mL) and sulfuric acid (15 mL) and mixture was heated under reflux for 10 min. Then, *N*-bromosuccinimide (12.5 g, 70.2 mmol) was slowly added to the mixture along a period of 5 h. The reaction mixture was then maintained under stirring at

ChemistryOpen

Research Article
doi.org/10.1002/open.202200007

Chemistry
Europe
European Chemical
Societies Publishing

60 °C for 48 h. Compound **6** was precipitated by cooling of the solution in an ice bath, filtered and dried under vacuum to get compound **6** (3 g, 35% yield), which does not require further purification. Spectral data were identical to those reported in reference.[63]

Synthesis of 3-(ethoxycarbonyl)phenyl boronic acid (**5**). Boronic acid **4** (6.7 g, 40.4 mmol) was dissolved in freshly distilled ethanol (30 mL) and then concentrated sulfuric acid (4.31 mL, 80.8 mmol) was added. The reaction mixture was heated at reflux overnight. Then, ethanol was evaporated and compound **5** (6 g, 90% yield) was obtained and used without further purification. ^{1}H NMR (400 MHz, CDCl$_3$), δ (ppm): 8.89 (s, 1H), 8.45 (dt, J_1=7.4 Hz, J_2= 1.3 Hz, 1H), 8.29 (dt, J_1=9.4 Hz, J_2=1.7 Hz, 1H), 7.62 (t, J=7.5 Hz, 1H), 4.47 (q, J=7.0 Hz, 2H), 1.47 (t, J=7.2 Hz, 3H).

Synthesis of ethyl 4′-bromo-2′,5′-bis(trifluoromethyl)-[1,1′-biphenyl]-3-carboxylate (**8**). Compound **6** (2.44 g, 6.56 mmol) and Cs$_2$CO$_3$ (4.27 g, 13.12 mmol) were dissolved in toluene/water (1:1, 200 mL). Boronic acid **5** (1.27 g, 6.56 mmol) and Pd(PPh$_3$)$_4$ (1.51 g, 1.31 mmol) were sequentially added. The reaction mixture was heated to reflux for 18 h. When the reaction was completed, the inorganic solids were removed by filtration through celite and washing with several portions of CH$_2$Cl$_2$ and the solvent was evaporated. The residue was purified by column chromatography using cyclohexane as eluent to give compound **8** as a white solid (2.9 g, 67%). ^{1}H NMR (400 MHz, CDCl$_3$), δ (ppm): 8.13 (bs, 1H), 7.64– 7.58 (m, 2H), 7.56–7.51 (m, 1H), 7.42–7.34 (m, 1H), 7.33–7.26 (m, 1H), 4.42 (q, J=7.2 Hz, 2H), 1.43 (t, J=7.2 Hz, 3H). We observe split signals due to two possible atropoisomers.

Synthesis of ethyl 4′-(4,4,5,5-tetramethyl-1,3,2-dioxaborolan-2-yl)-2′,5′- bis(trifluoromethyl)-[1,1′-biphenyl]-3-carboxylate (**3**). Under an argon atmosphere, a degassed solution of compound **8** (1.45 g, 3.51 mmol), bis(pinacolato)diboron (1.16 g, 4.56 mmol), Pd(dppf)$_2$Cl$_2$ (573 mg, 0.70 mmol) and potassium acetate (1.03 g, 10.53 mmol) in dry DME was refluxed for 12 h. After this period, the reaction was cooled to 20 °C, filtered, and diluted with CH$_2$Cl$_2$. The organic solution was washed with H$_2$O and brine, then dried with MgSO$_4$ and concentrated to dryness. The residue was separated by column chromatography (cyclohexane/EtOAc, 9:1) to give compound **3** as a white solid (918 mg, 54%). ^{1}H NMR (400 MHz, CDCl$_3$), δ (ppm): 8.31 (t, J=1.54 Hz, 1H), 8.17–8.10 (m, 1H), 8.06 (dt, J_1=8.01 Hz, J_2= 1,54 Hz, 1H), 8.00 (bs, 1H), 7.82 (ddd, J_1=7.86 Hz, J_2=3.08 Hz, J_3= 1.03 Hz, 1H), 7.57–7.50 (m, 1H), 4.42 (q, J=7.2 Hz, 2H), 1.43 (t, J= 7.2 Hz, 3H), 1.41 (s, 6H), 1.38 (s, 3H), 1.26 (s, 3H). ^{13}C NMR (100 MHz, CDCl$_3$), δ (ppm): 166.5, 140.5, 131.5, 131.2, 129.5, 129.0, 128.8, 128.3, 128.1, 85.1, 61.2, 29.8, 26.7, 24.6, 14.4.

Synthesis of tripodal compound **1**. Under argon atmosphere, compound **11**[58a] (422 mg, 0.53 mmol), compound **3** (780 mg, 1.60 mmol), Pd(PPh$_3$)$_4$ (368 mg, 0.318 mmol) and AgCO$_3$ (1.0 g, 4.24 mmol) were dissolved in dry THF. The mixture was stirred under argon atmosphere at 20 °C for 12 h. After this period, the reaction mixture was filtered through celite, washed with several portions of CH$_2$Cl$_2$ and the solvent was removed under vacuum. The product was purified by column chromatography (hexane/ EtOAc, 95:5) to yield **1** as a pale-yellow oil (375 mg, 52%). MALDI-TOF MS: m/z: calcd for C$_{75}$H$_{49}$BrF$_{18}$O$_6$Si [M+]: 1494.2194; found: 1494.2220. ^{1}H NMR (400 MHz, CDCl$_3$), δ (ppm): 8.16 (t, J=1.54 Hz, 1H), 8.15–8.13 (m, 3H), 8.12 (d, J=1.71 Hz, 1H), 8.08 (t, J=1.71 Hz, 2H), 8.02 (bs, 1H), 7.92 (bs, 2H), 7.90 (bs, 2H), 7.79 (bs, 1H), 7.77 (bs, 1H), 7.76 (bs, 1H), 7.73 (bs, 1H), 7.70–7.69 (m, 1H), 7.66–7. 64 (m, 1H), 7.62 (bs, 2H), 7.58 (bs, 2H), 7.56 (bs, 2H), 7.54 (bs, 1H), 7.53 (d, J=1.03 Hz, 1H), 7.52–7.51 (m, 4H), 7.49 - 7.45 (m, 4H), 7.40 (bs, 1H), 7.39 (bs, 1H), 7.38 (d, 1H), 4.42 (q, J=7.2 Hz, 6H), 1.42 (t, J=7.2 Hz, 9H). ^{13}C NMR (100 MHz, CDCl$_3$), δ (ppm): 166.1, 138.4, 133.8, 133.2,

131.7, 130.6, 130.1, 129.6, 129.0, 128.9, 128.2, 128.1, 127.1, 124.8, 124.6, 121.9, 61.3, 29.7, 14.3.

Interconversion of —COOEt groups to —COCl groups. Compound **1** (8 mg, 5.3 μmol) was dissolved in THF (2 mL) and then lithium hydroxide (3 м aqueous solution, excess) was added and reaction was stirred for 3 h at 20 °C. Then, the reaction mixture was acidified by addition of HCl 1.0 м until pH=3. Formation of triacid compound intermediate was confirmed by ^{1}H NMR spectroscopy. Then, reaction was concentrated under vacuum and dried. The crude was dissolved in thionyl chloride (3 mL) and heated at reflux overnight. Then, the solvent was evaporated and the residue was dried at high vacuum. Compound **1**-COCl was not isolated, it was directly used in the coupling with terminal amine-functionalized gold triangle nanoprisms.

Synthesis of (((4-bromophenyl)silanetriyl)tris([1,1′-biphenyl]-4′,3-diyl))trimethanol (**13**). Compound **12**[56] (950 mg, 1.29 mmol) was dissolved in anhydrous THF under argon atmosphere. Then glacial acetic acid (162 μL, 2.83 mmol) and 1.0 м solution of TBAF (2.83 mL, 2.83 mmol) were sequentially added and the reaction mixture was stirred at 20 °C for 6 h. Then, it was washed with water and extracted with CH$_2$Cl$_2$. The organic phase was washed with brine, dried over anhydrous MgSO$_4$, filtered and finally the solvent was removed under vacuum. The product was purified by column chromatography (EtOAc/Hexane 1:1 to MeOH as eluents) and then dried under vacuum to yield the triol compound **13** as a white solid (591 mg, 92%). ^{1}H NMR (400 MHz, CD$_3$OD), δ (ppm): 8.73–8.60 (m, 14H), 8.61–8.47 (m, 7H), 8.45–8.36 (m, 3H), 8.36–8.28 (m, 4H), 4.28 (bs, 6H, 3 x CH_2OH). ^{13}C NMR (100 MHz, CD$_3$OD), δ (ppm): 144.0, 143.8, 143.5, 142.2, 142.1, 139.2, 138.1, 138.0, 137.1, 134.5, 134.4, 133.7, 132.4, 130.0, 127.8, 127.7, 127.4, 127.1, 126.7, 65.2.

Synthesis of (((4-bromophenyl)silanetriyl)tris([1,1′-biphenyl]-4′,3-diyl))trimethanol, tripod **2**. Triphenylphosphine (357 mg, 1.36 mmol) was solved in anhydrous THF (30 mL) and then was cooled down at 0 °C, DIAD (268 μL, 1.36 mmol) was added and the reaction mixture was stirred for 30 min. Then, a solution of compound **13** (100 mg, 0.136 mmol) and thioacetic acid (97 μL, 1.36 mmol) was slowly added to the reaction mixture, which then was allowed to reach 20 °C under stirring for 5 h. After this period, the mixture was poured into water (20 mL) and extracted with ethyl acetate. The organic phase was washed with water, brine, dried over anhydrous MgSO$_4$, filtered, and concentrated to dryness under vacuum. Compound **2** was obtained after purification by column chromatography (gradient from cyclohexane/EtOAc 95:5 to 90:10) as a white solid. MALDI-TOF MS: m/z: calcd for C$_{51}$H$_{43}$BrO$_3$S$_3$Si [M+]: 906.1327; found: 906.1340. ^{1}H NMR (400 MHz, CDCl$_3$), δ (ppm): 7.70–7.60 (m, 13H), 7.58–7.48 (m, 10H), 7.39 (t, J=7.7 Hz, 3H), 7.32– 7.26 (m, 2H), 4.19 (s, 6H, 3 x CH$_2$S), 2.36 (s, 9H, 3 x C(O)CH$_3$). ^{13}C NMR (100 MHz, CDCl$_3$), δ (ppm): 195.1, 142.2, 141.3, 138.3, 137.9, 136.8, 136.5, 135.9, 132.5, 132.1, 131.2, 129.2, 128.6, 128.1, 127.7, 126.8, 126.2, 124.7, 33.6, 30.6.

Surface Modification

Preparation of amine and **1**-modified gold nanoprisms: Au@NTP-S-NH$_2$ and Au@NTP-S-NH-**1**. Gold nanotriangular prisms (Au@NTPs) were prepared by following the seedless procedure, using 3-butenoic acid (3BA) and benzyldimethyl ammonium chloride (BDAC), and separated from nanooctahedra by depletion-induced flocculation.[60] After re-dispersion of the Au@NTPs in a solution of BDAC (20 mL, 5 mм), 6-aminoalkanethiol (8 mg) was added to the suspension at 20 °C. After 30 min of slow stirring, the dispersion was centrifuged at 7500 rpm for 30 min, the supernatant was removed, and the residue was lyophilized (Au@NTP-S-NH$_2$). Then, a freshly prepared solution of tripodal compound **1**-COCl (8 mg,

ChemistryOpen

Research Article
doi.org/10.1002/open.202200007

Chemistry Europe
European Chemical
Societies Publishing

5.35 μmol) in ethanol (214 μL) was added to a solution prepared from lyophilized Au@NTP-S-NH$_2$ (2.5 mM, 2.14 mL) in absolute ethanol, and the mixture was stirred overnight at 20 °C. Then, the solvent was evaporated, and the residue was washed under sonication with distilled water and centrifuged. This process was repeated five times and finally, the residue was lyophilized.

Preparation of Au@NTP-S-**2**. A freshly prepared and degassed solution of tripodal compound **2** (10 mL, 80 μM in THF containing 30% v/v of a 1 M solution of triethylamine in THF) was added to a freshly prepared and degassed solution of Au@NTP (10 mL, 8 μM in water) and the mixture was strongly stirred during 48 h at 20 °C. Then, the organic solvent was evaporated, the residue was thoroughly washed with THF and ethanol (centrifugation), and the aqueous pellet was lyophilized to get Au@NTP-S-**2**.

Biocompatibility

Sample preparation for XPS study: in a 5 mL vial, Au@NTP, Au@NTP-S-**1** or Au@NTP-S-**2** (2 mg) lyophilized samples were immersed into a slowly stirred solution of fibrinogen (0.1%) in phosphate-buffered saline (PBS, 3 mL, 0.01 M, pH 7.4). The suspension was slowly stirred for 1 h at 30 °C. After this period, the samples were centrifuged, and then washed several times under a gentle flow of Millipore water for about 15 s. Finally, the pellet was dried under a stream of N$_2$ and subjected to XPS measurements. For previous analyses of protein adsorption and comparation purposes, pristine Au@NTP, Au@NTP-S-**1** or Au@NTP-S-**2** lyophilized pellets were analyzed by XPS.

Acknowledgements

Conflict of Interest

The authors declare no conflict of interest.

Data Availability Statement

The data that support the findings of this study are available from the corresponding author upon reasonable request.

[1] I. Banerjee, R. C. Pangule, R. S. Kane, *Adv. Mater.* **2011**, *23*, 690–718.
[2] a) L. Leoni, D. Attiah, T. A. Desai, *Sensors* **2002**, *2*, 111–120; b) S. Sharma, R. W. Johnson, T. A. Desai, *Appl. Surf. Sci.* **2003**, *206*, 218–229.
[3] P. C. Ke, S. Lin, W. J. Parak, T. P. Davis, F. A. Caruso, *ACS Nano* **2017**, *11*, 11773–11776.
[4] E. Ostuni, R. G. Chapman, R. E. Holmlin, S. Takayama, G. M. Whitesides, *Langmuir* **2001**, *17*, 5605–5620.
[5] C. Leng, S. Sun, K. Zhang, S. Jiang, Z. Chen, *Acta Biomater.* **2016**, *40*, 6–15.
[6] R. K. Kainthan, D. E. Brooks, *Biomaterials* **2007**, *28*, 4779–4787.
[7] Y. L. Li, L. Zhu, Z. Z. Liu, R. Cheng, F. H. Meng, J. H. Cui, S. J. Ji, Z. Y. Zhong, *Angew. Chem. Int. Ed.* **2009**, *48*, 9914–9918; *Angew. Chem.* **2009**, *121*, 10098–10102.
[8] E. Molena, C. Credi, C. De Marco, M. Levi, S. Turri, G. Simeone, *Appl. Surf. Sci.* **2014**, *309*, 160–167.
[9] C. D. Hodneland, Y.-S. Lee, D.-H. Min, M. Mrksich, *Proc. Nat. Acad. Sci. USA* **2002**, *99*, 5048–5052.
[10] B. T. Houseman, J. H. Huh, S. J. Kron, M. Mrksich, *Nat. Biotechnol.* **2002**, *20*, 270–274.
[11] J. C. Love, L. A. Estroff, J. K. Kriebel, R. G. Nuzzo, G. M. Whitesides, *Chem. Rev.* **2005**, *105*, 1103–1170.
[12] K. L. Prime, G. M. Whitesides, *Science* **1991**, *252*, 1164–1167.
[13] C. Hoffmann, G. E. M. Tovar, *J. Colloid Interface Sci.* **2006**, *295*, 427–435.
[14] D. J. Vanderah, G. Valincius, C. W. Meuse, *Langmuir* **2002**, *18*, 4674–4680.
[15] S.-W. Lee, P. E. Laibinis, *Biomaterials* **1998**, *19*, 1669–1675.
[16] A. Papra, N. Gadegaard, N. B. Larsen, *Langmuir* **2001**, *17*, 1457–1460.
[17] G. Qin, R. Zhang, B. Makarenko, A. Kumar, W. Rabalais, J. M. López-Romero, R. Rico, C. Cai, *Chem. Commun.* **2010**, *46*, 3289–3291.
[18] C. Bamdad, *Biophys. J.* **1998**, *75*, 1997–2003.
[19] D. C. Chow, W.-K. Lee, S. Zauscher, A. Chilkoti, *J. Am. Chem. Soc.* **2005**, *127*, 14122–14123.
[20] L. Wang, Q. Liu, R. M. Corn, A. E. Condon, L. M. Smith, *J. Am. Chem. Soc.* **2000**, *122*, 7435–7440.
[21] C. S. Chen, M. Mrksich, S. Huang, G. M. Whitesides, D. E. Ingber, *Science* **1997**, *276*, 1425–1428.
[22] R. McBeath, D. M. Pirone, C. M. Nelson, K. Bhadriraju, C. S. Chen, *Dev. Cell* **2004**, *6*, 483–495.
[23] S. Sekula, J. Fuchs, S. Weg-Remers, P. Nagel, S. Schuppler, J. Fraga, N. Theilacker, M. Franzreb, C. Wingren, P. Ellmark, C. A. K. Borrebaeck, C. A. Mirkin, H. Fuchs, S. Lenhert, *Small* **2008**, *4*, 1785–1793.
[24] J. C. Paulson, O. Blixt, B. E. Collins, *Nat. Chem. Biol.* **2006**, *2*, 238–248.
[25] R. L. Nicholson, M. Welch, M. Ladlow, *ACS Chem. Biol.* **2007**, *2*, 24–30.
[26] K. Y. Tomizaki, K. Usui, H. Mihara, *ChemBioChem* **2005**, *6*, 782–799.
[27] a) G. J. Leggett, *Analyst* **2005**, *130*, 259–264; b) N. L. Rosi, C. A. Mirkin, *Chem. Rev.* **2005**, *105*, 1547–1562.
[28] C. A. K. Borrebaeck, *Drug Discovery Today* **2007**, *12*, 813–819.
[29] D. Witt, R. Klajn, P. Barski, B. A. Grzybowski, *Curr. Org. Chem.* **2004**, *8*, 1763–1797.
[30] D. Coglitore, N. Giamblanco, A. Kizalaite, P. E. Coulon, B. Charlot, J.-M. Janot, S. Balme, *Langmuir* **2018**, *34*, 8866–8877.
[31] S. Schöttler, K. Landfester, V. Mailänder, *Angew. Chem. Int. Ed.* **2016**, *55*, 8806–8815; *Angew. Chem.* **2016**, *128*, 8950–8959.
[32] Q. Li, Y. Yan, M. Yu, B. Song, S. Shi, Y. Gong, *Appl. Surf. Sci.* **2016**, *367*, 101–108.
[33] S. H. Li, J. Y. Huang, M. Z. Ge, S. W. Li, T. L. Xing, G. Q. Chen, Y. Q. Liu, K. Q. Zhang, S. S. Al-Deyab, Y. K. Lai, *Mater. Des.* **2015**, *85*, 815–822.
[34] X. Yin, C. Sun, B. Zhang, Y. Song, N. Wang, L. Zhu, B. Zhu, *Chem. Eng. J.* **2017**, *330*, 202–207.
[35] L. D. Chambers, K. R. Stokes, F. C. Walsh, R. J. K. Wood, *Surf. Coat. Technol.* **2006**, *201*, 3642–3652.
[36] K. Page, M. Wilson, I. P. Parkin, *J. Mater. Chem.* **2009**, *19*, 3819–3831.
[37] H. Zhang, M. Chiao, *J. Med. Biol. Eng.* **2015**, *35*, 143–155.
[38] E. Molena, C. Credi, C. De Marco, M. Levi, S. Turri, G. Simeone, *Appl. Surf. Sci.* **2014**, *309*, 160–167.
[39] M. Yang, W. Liu, C. Jiang, C. Liu, S. He, Y. Xie, Z. Wang, *J. Mater. Sci.* **2019**, *54*, 2079–2092.
[40] H. S. Sundaram, Y. Cho, M. D. Dimitriou, J. A. Finlay, G. Cone, S. Williams, D. Handlin, J. Gatto, M. E. Callow, J. A. Callow, *ACS Appl. Mater. Interfaces* **2011**, *3*, 3366–3374.
[41] C. Leng, H. G. Buss, R. A. Segalman, Z. Chen, *Langmuir* **2015**, *31*, 9306–9311.
[42] Z. Zhao, H. Ni, Z. Han, T. Jiang, Y. Xu, X. Lu, P. Ye, *ACS Appl. Mater. Interfaces* **2013**, *5*, 7808–7815.
[43] R. E. Baier, *J. Mater. Sci. Mater. Med.* **2006**, *17*, 1057–1062.
[44] C. Carrillo-Carrión, M. Atabakhshi-Kashi, M. Carril, K. Khajeh, W. J. Parak, *Angew. Chem. Int. Ed.* **2018**, *57*, 5033–5036; *Angew. Chem.* **2018**, *130*, 5127–5130.
[45] C. Carrillo-Carrión, M. Gallego, W. J. Parak, M. Carril, *Materials* **2018**, *11*, 750–759.
[46] M. Carril, D. Padro, P. Del Pino, C. Carrillo-Carrión, M. Gallego, W. J. Parak, *Nat. Commun.* **2017**, *8*, 1542.

ChemistryOpen

Research Article
doi.org/10.1002/open.202200007

Chemistry Europe
European Chemical
Societies Publishing

[47] Y. X. Yao, J. M. Tour, *J. Org. Chem.* **1999**, *64*, 1968–1971.

[48] Y. Shirai, J. M. Guerrero, T. Sasaki, T. He, H. Ding, G. Vives, B. Yu, C. Cheng, A. K. Flatt, P. G. Taylor, Y. Gao, J. M. Tour, *J. Org. Chem.* **2009**, *74*, 7885–7897.

[49] S. Thyagarajan, A. Liu, O. A. Famoyin, M. Lamberto, E. Galoppini, *Tetrahedron* **2007**, *63*, 7550–7559.

[50] M. Lamberto, C. Pagba, P. Piotrowiak, E. Galoppini, *Tetrahedron Lett.* **2005**, *46*, 4895–4899.

[51] C.-H. Lee, Y. Zhang, A. Romayanantakit, E. Galoppini, *Tetrahedron* **2010**, *66*, 3897–3903.

[52] Y. S. Choi, C. W. Yoon, H. D. Lee, M. Park, J. W. Park, *Chem. Commun.* **2004**, 1316–1317.

[53] D. Deluge, C. Cai, *Langmuir* **2005**, *21*, 1917–1922.

[54] X. Deng, A. Mayeux, C. Cai, *J. Org. Chem.* **2002**, *67*, 5279–5283.

[55] J. Hierrezuelo, E. Guillén, J. M. López-Romero, R. Rico, M. R. López-Ramírez, J. C. Otero, C. Cai, *Eur. J. Org. Chem.* **2010**, 5672–5680.

[56] R. Suau, R. Rico, F. Najera, F. J. Ortiz-López, J. M. López-Romero, M. Moreno-Mañas, A. Roglans, *Tetrahedron* **2004**, *60*, 5725–5735.

[57] P. Horcajada, F. Salles, S. Wuttke, T. Devic, D. Heurtaux, G. Maurin, A. Vimont, M. Daturi, O. David, E. Magnier, N. Stock, Y. Filinchuk, D. Popov, C. Riekel, G. Férey, C. Serre, *J. Am. Chem. Soc.* **2011**, *133*, 17839–17847.

[58] a) M. Sánchez-Molina, J. M. López-Romero, J. Hierrezuelo-León, M. Martín-Rufián, A. Díaz, M. Valpuesta, R. Contreras-Cáceres, *Asian J. Org. Chem.* **2016**, *5*, 550–559; b) J. Hierrezuelo, R. Rico, M. Valpuesta, A. Díaz, J. M. López-Romero, M. Rutkis, J. Kreigberga, V. Kampars, M. Algarra, *Tetrahedron* **2013**, *69*, 3465–3474.

[59] M. A. Casado-Rodríguez, M. Sánchez-Molina, A. Lucena-Serrano, C. Lucena-Serrano, B. Rodríguez-González, M. Algarra, A. Díaz, M. Valpuesta, J. M. López-Romero, J. Pérez-Juste, R. Contreras-Cáceres, *Nanoscale* **2016**, *8*, 4557–4564.

[60] A. B. Ruiz-Muelle, C. Kuttner, C. Alarcón-Fernández, J. M. López-Romero, P. Uhlmann, R. Contreras-Cáceres, I. Fernández, *Appl. Surf. Sci.* **2019**, *496*, 143598.

[61] a) M. Sánchez-Molina, A. Díaz, E. Sauter, M. Zharnikov, J. M. López-Romero, *Appl. Surf. Sci.* **2019**, *470*, 259–268; b) M. Lindner, M. Valasek, J. Homberg, K. Edelmann, L. Gerhard, W. Wulfhekel, O. Fuhr, T. Wätcher, M. Zharnikov, V. Kolivoska, L. Pospisil, G. Meszaros, M. Hromadova, M. Mayor, *Chem. Eur. J.* **2016**, *22*, 13218.

[62] M. Sánchez-Molina, A. Díaz, M. Valpuesta, R. Contreras-Cáceres, J. M. López-Romero, M. R. López-Ramírez, *Appl. Surf. Sci.* **2018**, *445*, 175–185.

[63] R. Suau, R. Rico, J. M. López-Romero, F. Nájera, A. Ruiz, F. J. O. López, *ARKIVOC* **2002**, *v*, 64–72.